Journal of Innovative Optical Health Sciences
Vol. 2, No. 1 (2009) 107–115

World Scientific
www.worldscientific.com

EFFICIENT FITTING RANGE FOR GLUCOSE MEASUREMENT WITH OPTICAL COHERENCE TOMOGRAPHY

SHU FENG, KEHONG YUAN and DATIAN YE*

Graduate School at Shenzhen & Department of Biomedical Engineering
Tsinghua University, China
**yedt6386@sz.tsinghua.edu.cn*

Studies of non-invasive glucose measurement with optical coherence tomography (OCT) in tissue-simulating phantoms and biological tissues show that glucose has an effect on the OCT signal slope. Choosing an efficient fitting range to calculate the OCT signal slope is important because it helps to improve the precision of glucose measurement. In this paper, we study the problem in two ways: (1) scattering-induced change of OCT signal slope versus depth in intralipid suspensions with different concentrations based on Monte Carlo (MC) simulations and experiments and (2) efficient fitting range for glucose measurement in 3% and 10% intralipid. The results show that the OCT signal slope expresses a contrary change with scattering coefficient below a certain depth in high intralipid concentrations, so that there is an effective fitting depth. With an efficient fitting range from 100 μm to the effective fitting depth, the precision of glucose measurement can be 4.4 mM for 10% intralipid and 2.2 mM for 3% intralipid.

Keywords: Optical coherence; tomography; noninvasive glucose measurement; multiple scattered photons.

1. Introduction

Non-invasive measurement of the glucose concentration of the human body based on optical techniques has been developed during the past 20 years. Optical coherence tomography (OCT) was proposed by Huang *et al.*[1] as a new technique for high-resolution imaging based on the detection of light backscattered from tissue and further analyzed in respect to its applicability for non-invasive glucose monitoring by Esenaliev *et al.*[2] and Larin *et al.*[3] The measurement relies on the glucose-induced change of OCT signal slope which is calculated by linear fitting with a certain range; hence, the study of the efficient fitting range is significant to improve the accuracy of glucose measurement.

Increasing glucose concentration decreases the refractive index mismatch between the scattering particles and the base medium, and thus reduces the scattering coefficient.[4] The OCT signal slope is demonstrated to express the glucose-induced change of scattering coefficient by simulations and experiments in tissue-simulation phantoms, *in vitro* and *in vivo*. Kirillin *et al.*[5] show a 7%/ 56 mM change in simulations for 5% intralipid. Kinnunen *et al.*[6] show a 2.1%/ 30 mM change in 2% intralipid and a 0.86%/ 30 mM change in 5% intralipid. Their study *in vitro* also shows changes between 20% and 52%/ 30 mM in different mouse skin samples. Larin *et al.* show a 0.023%/ mM change in polystyrene microsphere suspension and a 0.032%/ mM change in 3% fat milk.[7] Their study

in vivo also shows a 3.3%/ mM change in the rabbit ear, a 2.3%/ mM change in the micropig skin,[8] and a change of 3.4%/mM in human subjects.[9] It was shown that the OCT technique has several advantages over other optical methods proposed for non-invasive measurement and monitoring of tissue optical properties such as high resolution and capability of probing specific tissue layers. However, various fitting range are used to calculate the OCT signal slope in their experiments. Kirillin *et al.* and Kinnunen *et al.* chose the fitting range where the linear dependence was most clear. Larin *et al.* chose the range of 300–400 μm for the rabbit ear, 260–400 μm for the micropig skin, 550–600 μm, and 380–500 μm for forearm skin of human body. Different fitting range leads to different change and accuracy of OCT signal slope, as a result, the precision of glucose measurement is different. As to which can be an efficient fitting range has not been discussed in their researches.

In order to choose an efficient fitting range, it is necessary to better understand the scattering-induced changes of OCT signal slope versus depth in a highly scattering medium. The single scattering model describes the OCT signal as the probing light into the tissue being continuously attenuated according to the total extinction coefficient of the propagation medium.[10] It was then quickly realized that this model appears to give an incomplete description of beam propagation progressing deep into the tissues where the multiple scattering effect can no longer be neglected.[11] For glucose sensing in human body, OCT technique measures glucose-induced changes of scattering coefficient in the dermis layer of skin, where the multiple scattering photons (MSPs) play a non-negligible role. A model also taking into account MSPs could be more preferable.

Monte Carlo (MC) simulation has been proven to be an accurate method to study photon-tissue interaction. MC simulation provides a statistical method for implementing realistic models of the experimental situations based on specific geometries, characteristic parameters of source and detector, as well as stochastic modeling of light propagation in the scattering medium. Smithies *et al.*[12] developed an MC model according to their specific OCT system geometry to investigate how signal attenuation and localization are influenced by multiple scattering effects. In the meantime, Yao and Wang[13] developed an MC model to simulate how multiple scattering degrades the OCT signal attenuation into the tissue, by separate considerations of the least scattering and MSPs. Despite these advances, an investigation of the scattering-induced change of OCT signal slope versus depth is still lacking so far.

In this study, we applied MC simulation taking into account MSPs and experiments to study the scattering-induced changes of OCT signal slope versus depth in intralipid suspensions with different concentrations. We also studied the efficient fitting range for glucose measurement in 3% and 10% intralipid.

2. Materials and Methods

2.1. *MC simulation*

In OCT, the low-coherence interference modulation is equal to the product of mutual correlation of two functions,[14]

$$Id(Lr) = 2(IsIr)^{1/2}[R^{1/2}(Ls) \otimes C(Ls)] \qquad (1)$$

where I_s and I_r are the signal intensities in the sample and reference arms respectively, L_r and L_s are the corresponding path lengths of I_s and I_r, $\otimes$ denotes convolution, $C(L_s)$ is the self-coherence function of the light source, $R(L_s) = [dI_s(L_s)/dL_s]/I_s$ is the pathlength-resolved diffuse reflectance of the sample, which is the key of the OCT signal. The aim of MC simulation is to obtain $R^{1/2}(L_s)$.

The MC program was modified according to Wang *et al.*[15] to take into account the OCT principle. Each individual photon launched from the probe was propagated into the medium, while accounting for its accumulated pathlength and the number of scattering events. At each interaction within the medium, the scattering angle was determined by stochastically sampling the Henyey–Greenstein phase function. For each interaction, the position of the scattering event was recorded; the accumulated pathlength was increased by the length of the latest path segment. The propagation of any photon was terminated if it exits the medium outside the probe radius r and probe angle θ as shown in Fig. 1, or half of its accumulated pathlength exceeds the maximum prespecified depth to be monitored. If the photon exits within the probe area, its history and scattering events will be recorded. To ease the simulations, it was assumed that the probe is in direct contact with the turbid medium. For simplicity, the incident light from the probe was assumed to be a pencil beam.

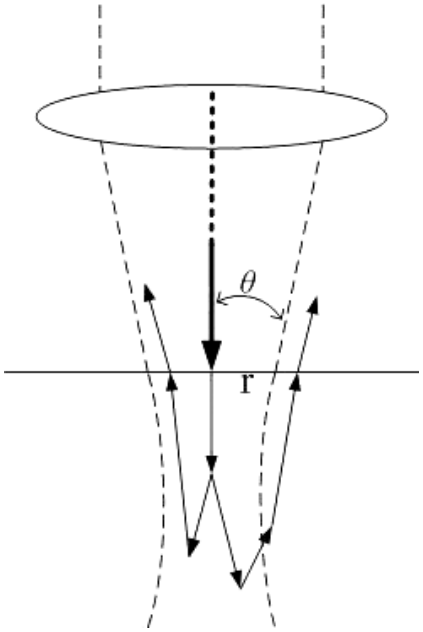

Fig. 1. The MC simulation model of OCT.

The specular reflection from the air-tissue interface was neglected in the simulations.

In this simulation, $r = 30$ and $\theta = 5°$, which can be altered according to different numerical aperture (NA) of the objective lens. According to the formulas of scattering coefficient μ_s and anisotropy factor g of standard 10% intralipid proposed by Staveren *et al.*,[16] and g of C% intralipid was estimated: $\mu_s = 8.4\,\mathrm{Ccm}^{-1}$ and $g = 0.34$. Based on Ref. 17, refractive index n of water was chosen as 1.32. Absorption coefficient $\mu_a = 1\,\mathrm{cm}^{-1}$ was assumed. Concentrations of 1%–10% were studied. The total number of incident photons used in each simulation was 10^9.

2.2. *Measurement system*

The OCT system with a grating-based rapid-scanning optical delay (RSOD) line used in our studies is depicted in Fig. 2. The RSOD line that employs phase control has several advantages, including high-speed, high-duty cycle, phase- and group-delay independence, and group-velocity dispersion compensation.[18] We used a superluminescent diode (SLD) with the center wavelength of 1310 nm and the full-width at half-maximum (FWHM) spectral width of 40 nm as a light source. The output power of SLD was 1 mW. The emitted radiation was coupled into a single-mode fiber-optic Michelson interferometer. The light was split by a 4×2 coupling module into sample and reference arms and then reflected back, respectively. The 4×2 coupling module consisted of one 2×2 beam splitter (50:50) and two 1×2 beam splitters (50:50). The reflected beam from reference arm and sample arm was recombined at the coupling module, producing an interference pattern when the difference between their pathlengths is smaller than the coherence length of the light source. In-depth scanning with a frequency of 100 Hz was produced electronically by galvanometer mirror in the reference arm. The generated interference signal is detected by two photodiodes, differential amplified to suppress background light noise, electronically filtered around the modulation frequency ($f = 36\,\mathrm{kHz}$), digitized by a 12-bit data acquisition card (National Instruments type PCI6111), and recorded by a computer for further processing. The actual axial and lateral resolutions of our OCT system were measured as 22 μm and 18 μm, respectively.

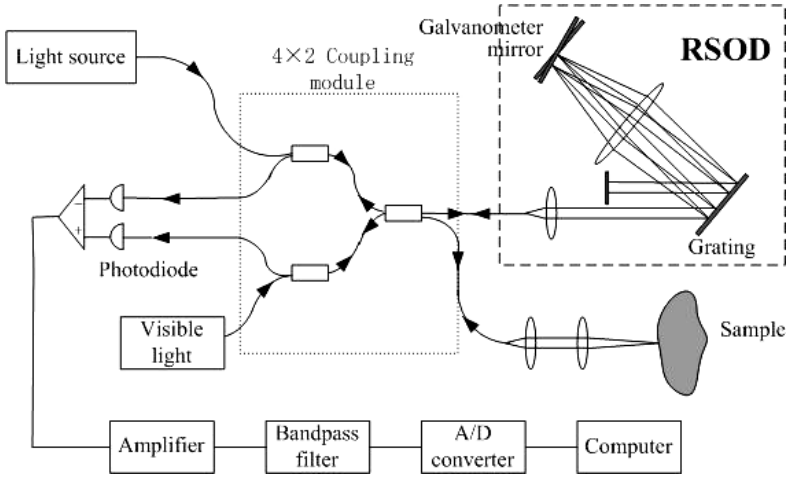

Fig. 2. Schematics of OCT system with grating-based RSOD line used in the experiment.

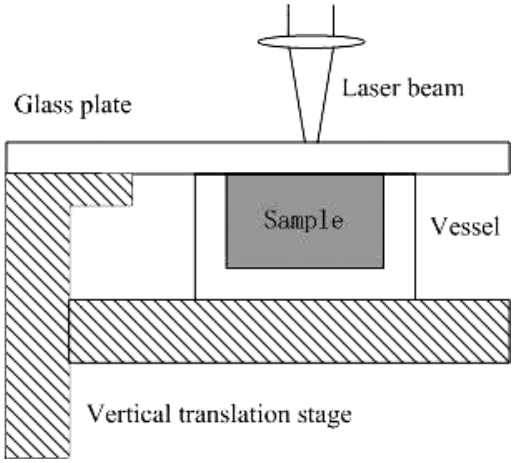

Fig. 3. Schematics of sample set-up.

The probe depth was 1400 μm into intralipid samples. Nearly 10,000 scans are applied to each measurement with 100 seconds. Each sample was measured 5 times, and the average and standard deviation (SD) were calculated.

The sample set-up shown in Fig. 3 was used to avoid the influence of confocal function[19] and DC component. The glass plate (a standard 1 mm-thick microscope slide) was stuck on the fixed bracket. The vessel was filled with sample suspension and put on a vertical translation stage. The intralipid suspension surface was higher than the edge of the vessel due to the tension of the liquid surface. The stage was adjusted to the very position such that the surface of the sample suspension was just touching the glass plate. This set-up keeps the surface of sample suspension at the same probe depth during all the experiments.

2.3. *Materials*

Intralipid suspensions are widely used as a tissue-simulating phantom in biomedical research, chiefly because their scattering properties resemble those of skin tissue. Experiments were performed with concentrations of 1%–10%. Samples were prepared by adding distilled water to 20% intralipid solution. The constituents of intralipid 20%, according to the manufacturer, are: soybean oil 20%, lecithin 1.2%, glycerin 2.2%, and water 76.6%. We also used 3% and 10% intralipid as scattering medium with different scattering properties. Glucose concentrations (500, 1000, 1500, 2000, 2500, 3000, 3500, 4000, 4500, and 5000 mg/dL) were used to study the change of OCT signal slope. These glucose concentrations were chosen because the effect of glucose on the optical properties is quite small in intralipid suspension.

3. Results

3.1. *Scattering-induced change of OCT signal slope versus depth*

Simulated $R^{1/2}(L_s)$ and experimental OCT signal from intralipid suspensions are shown in Fig. 4. One can see that an increasing scattering coefficient causes two kinds of changes. First, more backscattered photons are detected from the surface; second, the OCT signal has larger slope in low depth. However, in high concentrations, the scattering-induced change of slope decreases with an increasing depth, and has a contrary phenomenon below a certain depth. As it can be seen, the slope of 8% intralipid is larger than that of 10% intralipid

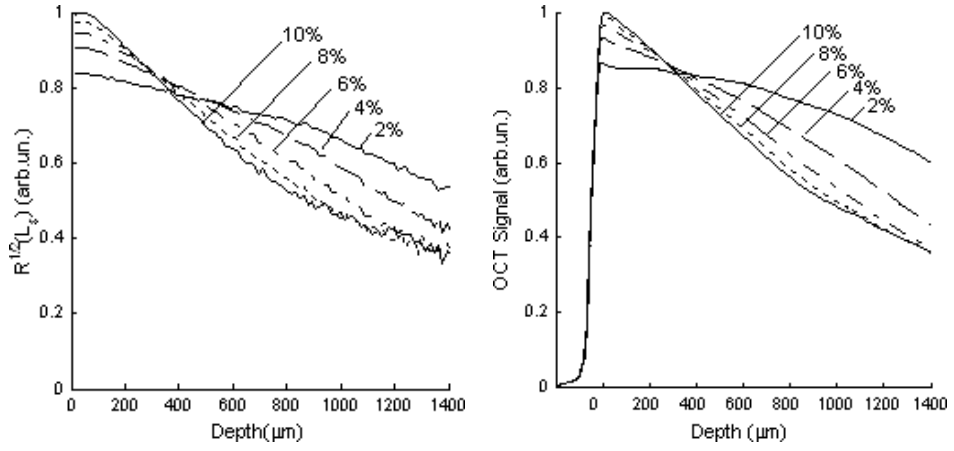

(a) (b)

Fig. 4. (a) Simulated pathlength-resolved diffuse reflectance and (b) experimental OCT signal in logarithm as a function of depth in intralipid suspensions with different concentrations.

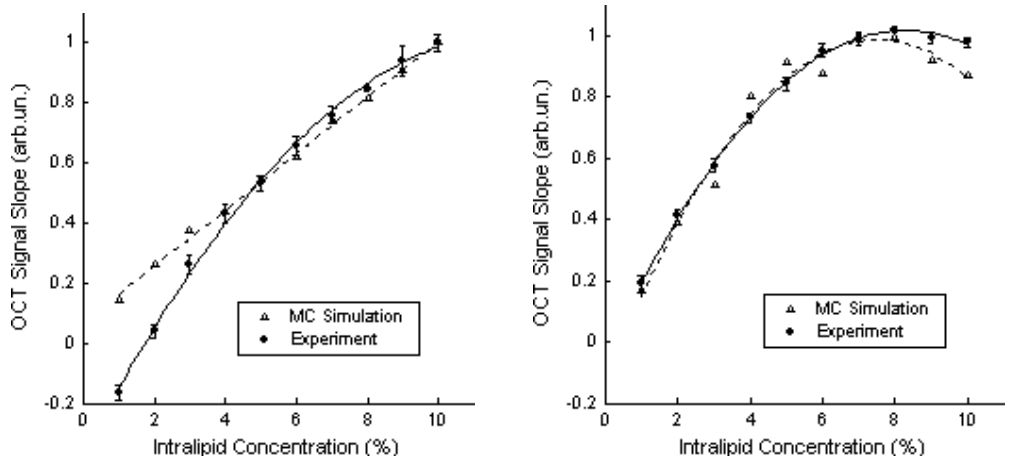

Fig. 5. Simulated and experimental OCT signal slope as a function of intralipid concentration calculated between the range: (a) 100–200 μm and (b)700–800 μm.

below approximately 600 μm in simulated $R^{1/2}(L_s)$ and approximately 700 μm in experimental OCT signal. The difference between simulations and experiments can be due to the simplification of the simulation model and difference between the parameters used in simulations and the practical one.

Figure 5(a) shows the simulated and experimental OCT signal slope (S_{OCT}) as a function of intralipid concentration calculated between the range 100–200 μm. Each S_{OCT} was calculated by a linear function $y = S_{\mathrm{OCT}}\,x + b$, where y is the magnitude of OCT signal in logarithm and x is the depth, using the least-square method. The relationship between S_{OCT} and concentration is almost linear in simulation results, however, a quadratic fitting gives a better correction in experiment results. This is due to the quadratic behavior of scattering coefficient and concentration as previously mentioned by Zaccanti *et al.*[20] Figure 5(b) shows the simulated and experimental OCT signal slope (S_{OCT}) as a function of intralipid concentration calculated between the range 700–800 μm. S_{OCT} and intralipid concentration can be well fitted with quadratic functions. As can be seen, the scattering-induced change of S_{OCT} is obvious in low concentrations, but undistinguishable in high concentrations. It is reasonable to point out that S_{OCT} at the range 700–800 μm from 8%, 9% and 10% intralipid, shows a contrary change.

3.2. *Efficient fitting range of glucose measurement*

Increasing the amount of glucose reduces the mismatch between scattering particles and the aqueous media and hence decreases the scattering coefficient. As a consequence, the OCT signal slope decreases within the effective fitting depth, which can be seen from Fig. 6. The experimental OCT signals for 10% and 3% intralipid with glucose concentrations of 500 mg/dL and 5000 mg/dL, respectively are presented. The glucose-induced change of OCT signal can be clearly observed. The effective fitting depth is 730 μm in 10% intralipid, which is calculated by getting the position of extremum from the subtraction of the two signals, and the effective fitting depth is the whole probe range in 3% intralipid.

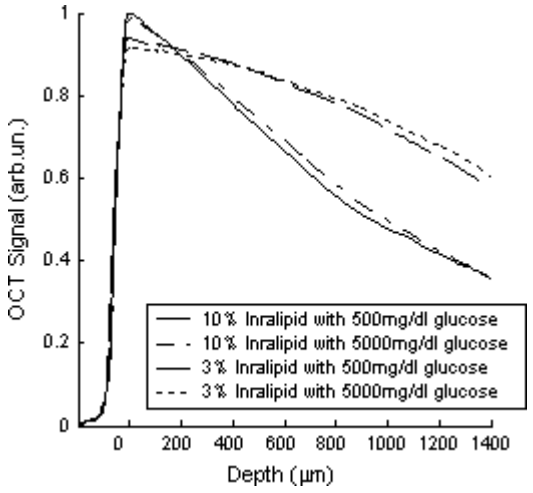

Fig. 6. Experimental OCT signals in logarithm from 3% and 10% intralipid with different glucose concentrations.

The fitting range was chosen below 100 μm for a greater similarity with the glucose sensing in the dermis layer of the human skin. First, we

chose the fitting range 100–300 μm where the linear dependence is most clear. The dependence of S_{OCT} on the glucose concentration in 3% and 10% intralipid is shown in Fig. 7(a) and 7(c) respectively. The S_{OCT} in Fig. 7 was normalized by that calculated at the range 100–200 μm in 10% intralipid. The glucose-induced change of scattering coefficient is quite small, therefore, S_{OCT} and glucose concentration can be well-fitted with linear function. The average glucose-induced change of S_{OCT} is $0.25 \times 10^{-3}\,\mathrm{mM}^{-1}$ in 3% intralipid and $0.45 \times 10^{-3}\,\mathrm{mM}^{-1}$ in 10% intralipid. Secondly, we chose the fitting range from 100 μm to the effective fitting depth. The dependence of S_{OCT} on the glucose concentration in 3% and 10% intralipid is shown in Figs. 7(b) and (d), respectively. The average glucose-induced change of S_{OCT} is $0.25 \times 10^{-3}\,\mathrm{mM}^{-1}$ in 3% intralipid and $0.37 \times 10^{-3}\,\mathrm{mM}^{-1}$ in 10% intralipid. However, a rather small SD can be seen in the plots.

We calculated S_{OCT} of every scan, and then got the statistic characteristics of S_{OCT} after averaging of 50,000 scans, as shown in Table 1, ΔZ is the fitting range, SEM is the standard error of the mean, ΔS_{OCT} is glucose-induced change of S_{OCT}. One can see from Table 1 that S_{OCT} at fitting range 100–730 μm has a $\frac{1}{5.4}$ SEM in comparison with 100–300 μm despite of a little smaller change in 10% intralipid. The S_{OCT} at fitting range 100–1400 μm has a $\frac{1}{16}$ SEM in comparison with 100–300 μm, and also has a same change in 3% intralipid. The range from 100 μm to the effective fitting depth shows to be efficient for glucose measurement.

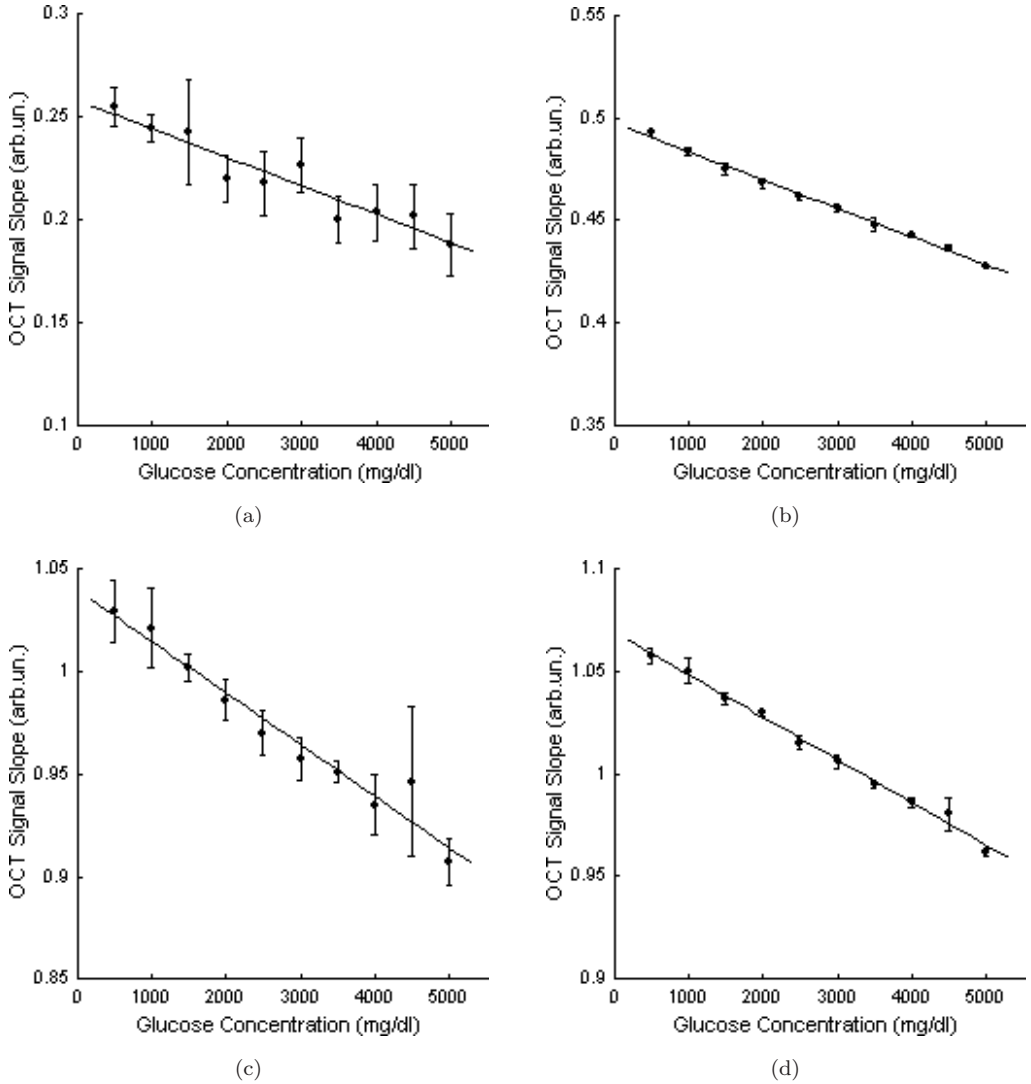

Fig. 7. Experimental OCT signal slope as a function of glucose concentration calculated at the range: (a) 100–300 μm (b) 100–1400 μm from 3% intralipid, and at the range (c) 100-300 μm (d) 100–730 μm from 10% intralipid.

Table 1. Statistical characteristics of OCT signal slope.

Samples	ΔZ (μm)	S_{OCT}	SD	SEM (10^{-3})	ΔS_{OCT} (10^{-3}/ mM)
Intralipid 10%	100–300	1.04	0.98	4.4	0.45
Intralipid 10%	100–730	1.07	0.18	0.81	0.37
Intralipid 3%	100–300	0.29	0.98	4.4	0.25
Intralipid 3%	100–1400	0.53	0.061	0.27	0.25

4. Discussions

As shown in the simulation result in Fig. 5(a), the fitting conic is almost after the origin, that is, when the backscattering coefficient is zero, the slope equals zero. But in the experimental results, the OCT signal slope in 1% intralipid is under zero, because the confocal function made the light intensity detected at the focal plane larger, which was adjusted at a depth approximately 400 μm in the experiment, and the DC component made the light intensity detected from the lower depth larger in our OCT system. The set-up in Fig. 3 could keep focal plane at the same depth, and make the DC component consistent with probe depth into samples during the experiment, so that there is no effect on the scattering-induced change of slope.

The scattering-induced change of S_{OCT} decreases with an increasing fitting depth in high intralipid concentrations, but almost the same with increasing fitting depth in low intralipid concentrations, which can be explained in Fig. 8. The plots for the single-scattered photons (SSP) and multiple scattered photons (MSP) signals separately from 3% and 10% intralipid are presented. It can be seen that the signal of SSP has almost a linear relationship with the depth, but the signal of MSP has a complicated form. The scattering-induced change of MSP signal slope is clear in low depth, but cannot be distinguished in large depth. The SSP signal is dominant within the whole probe depth in 3% intralipid, and the MSP signal is dominant below 60 μm in 10% intralipid. Therefore, the decreasing change of OCT signal slope with increasing depth in high concentrations is due to the dominant MSP signal, and the same change in low concentrations is due to the dominant SSP signal.

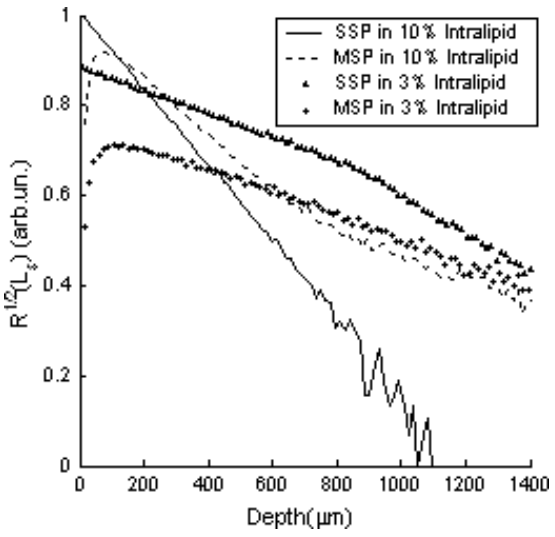

Fig. 8. Simulated pathlength-resolved diffuse reflectance for the SSP and MSP as function of depth from 3% and 10% intralipid.

The effect of glucose on the scattering properties of intralipid has been studied by Kinnunen *et al.*[6] Their results show that the relative value of glucose-induced change of OCT signal slope ($\Delta S_{\mathrm{OCT}}/S_{\mathrm{OCT}}$) is larger in 2% intralipid (0.07% mM^{-1}) than in 5% intralipid (0.029% mM^{-1}). Our results show that a $0.25\times10^{-}3\,\mathrm{mM}^{-1}$ change with a relative value of 0.086% mM^{-1} in 3% intralipid and a $0.45\times10^{-3}\,\mathrm{mM}^{-1}$ change with a relative value of 0.043% mM^{-1} in 10% intralipid when the fitting range 100–300 μm was chosen. The relative value is also larger in lower concentration in our experiments; however, the relative value from 10% intralipid is larger than the result from 5% intralipid, and the relative value from 3% intralipid is larger than their result from 2% intralipid. In our opinion, the confocal function and DC component mentioned above are the most important factors except for the different fitting ranges and wavelengths. We also mentioned that the absolute change of slope is larger in 10% intralipid than in 3% intralipid, showing that the absolute change of scattering coefficient is larger in 10% intralipid than in 3% intralipid, which can be explained by Mie scattering theory.

According to the statistics, for 95% confidence interval, one needs to use the width of this interval of approximately ±2 SEM. Therefore, assuming that the systematic error is negligible compared to the statistical error, when

the efficient fitting range from $100\,\mu$m to the effective fitting depth is used, the glucose concentration can be measured with a precision of approximately $\pm 2\,\mathrm{SEM}/\Delta S_{\mathrm{OCT}} = \pm 4.4\,$mM in 10% intralipid and $\pm 2.2\,$mM in 3% intralipid. We also mentioned that the precision of glucose measurement in 3% intralipid can be improved by applying a larger probe depth. Since the effective fitting depth decreases with the square root of the number of independent scans used for averaging, the precision of glucose measurement can be improved by applying a higher scanning frequency in the limited acquisition time.

As can be seen from Fig. 4, the effective fitting depth increases with decreasing μ_s. We also found that the effective fitting depth increases with increasing g by MC simulations, which is not given here. A light with longer center wavelength has a smaller μ_s and a larger g in tissue.[21] Hence, using a light source with longer center wavelength in OCT could bring a larger effective fitting depth. Additionally, higher-depth resolution can reduce the distortion of OCT signal caused by multiple scattering, as a result, this could lead to a larger efficient fitting depth. Our future work will be focused on the points proposed above.

5. Conclusions

Our results show that the OCT signal slope expresses a contrary change with scattering coefficient below a certain depth in high intralipid concentrations, so that there is an effective fitting depth. The precision of glucose measurement can be $\pm 4.4\,$mM for 10% intralipid and $\pm 2.2\,$mM for 3% intralipid when the fitting range is $100\,\mu$m to the effective fitting depth. The results suggest that the effective fitting depth should be considered when choosing an efficient fitting range for glucose measurement with OCT in tissue.

References

1. Huang, D., Swanson, E. A., Lin, C. P., Schuman, J. S., Stinson, W. G., Chang, W., Hee, M. R., Flotte, T., Gregory, K., Puliato, C. A. and Fujimoto, J. G., "Optical coherence tomography," *Sci.* **254**, 1178–1181 (1991).
2. Esenaliev, R. O., Larin, K. V., Larina, I. V. and Motamedi, M., "Noninvasive monitoring of glucose concentration with optical coherence tomography," *Opt. Lett.* **26**, 992–994 (2001).
3. Larin, K., Larina, I., Motamedi, M., Gelikonov, V., Kuranov, R. and Esenaliev, R., "Potential application of optical coherence tomography for noninvasive monitoring of glucose concentration," in: A. V. Priezzhev and G. L. Cot (eds.), *Optical Diagnostics and Sensing of Biological Fluids and Glucose and Cholesterol Monitoring, Proc. SPIE* **4263**, 83–90 (2001).
4. Kohl, M., Cope, M., Essenpreis, M. and Bocker, D., "Influence of glucose concentration on light scattering in tissue-simulating phantoms," *Opt. Lett.* **19**, 2170–2172 (1994).
5. Kirillin, M., Priezzhev, A. V., Kinnunen, M., Alarousu, E., Zhao, Z., Hast, J. and Myllylä, R., "[a]Glucose sensing in aqueous Intralipid suspension with an optical coherence tomography system: experiment and Monte Carlo simulation," in: G. L. Cote and A. V. Priezzhev (eds.), *Optical Diagnostics and Sensing IV, Proc. SPIE* **5325**, 164–173, (2004).
6. Kinnunen, M., Myllylä, R., Jokela, T. and Vainio, S., "*In vitro* studies toward noninvasive glucose monitoring with optical coherence tomography," *Appl. Opt.* **45**, 2251–2260 (2006).
7. Larin, K. V., Ashitkov, T. V., Larina, I., Petrova, I., Eledrisi, M., Motamedi, M. and Esenaliev, R. O., "Optical coherence tomography and noninvasive blood glucose monitoring: a review," in: V. V. Tuchin (eds.), *Optical Technologies in Biophysics and Medicine* V, *Proc. SPIE* **5474**, 285–290 (2004).
8. Larin, K. V., Motamedi, M., Ashitkov, T. V. and Esenaliev, R. O., "Specificity of non-invasive blood glucose sensing using optical coherence tomography technique: a pilot study," *Phys. Med. Biol.* **48**, 1371–1390 (2003).
9. Larin, K. V., Motamedi, M., Eledrisi, M. S. and Esenaliev, R. O., "Noninvasive blood glucose monitoring with optical coherence tomography, a pilot study in human subjects," *Diabetes Care* **25**, 2263–2267 (2002).
10. Schmitt, J. M., Knuttle, A. and Bonner, R. F., "Measurement of optical properties of biological tissues by low coherence interferometry," *Appl. Opt.* **32**, 6032–6042 (1993).
11. Yadlowsky, M. J., Schmitt, J. M. and Bonner, R. F., "Multiple scattering in optical coherence microscopy," *Appl. Opt.* **34**, 5699–5707 (1995).
12. Smithies, D. J., Lindmo, T., Chen, Z., Nelson, J. S. and Miller, T., "Signal attenuation and localisation in optical coherence tomography by Monte Carlo simulation," *Phys. Med. Biol.* **43**, 3025–3044 (1998).
13. Yao, G. and Wang, L. V., "Monte Carlo simulation of an optical coherence tomography signal in homogeneous turbid media," *Phys. Med. Biol.* **44**, 2307–2320 (1999).
14. Pan, Y. T., Birngruber, R., Rosperich, J. and Engelhardt, R., "Low-coherence optical tomography in

turbid tissue: theoretical analysis," *Appl. Opt.* **34**, 6564–6574 (1995).
15. Wang, L. H., Jacques, S. J. and Zheng, L. Q., "MCML–Monte Carlo modeling of photon transport in multi-layered tissue," *Comput. Methods Programs Biomed.* **47**, 131–146 (1995).
16. van Staveren, H. G., Moes, C. J. M., van Marle, J., Prahl, S. A. and van Gemert, M. J. C., "Light scattering in Intralipid-10% in the wavelength range of 400-1100 nm," *Appl. Opt.* **30**, 4507–4514 (1991).
17. George M. H. and Marvin, R. Q., "Optical constants of water in the 200 nm to 200 μm wavelength region," *Appl. Opt.* **12**, 555–563 (1973).
18. Tearney, G. J., Bouma, B. E. and Fujimoto, J. G., "High-speed phase- and group-delay scanning with a grating-based phase control delay line," *Opt. Lett.* **22**, 1811–1813 (1997).
19. Kholodnykh, A. I., Petrova, I. Y., Larin, K. V., Motamedi, M. and Esenaliev, R. O., "Optimization of low coherence interferometry for quantitative analysis of tissue optical properties," in: A. V. Priezzhev and G. L. Cot (eds.), *Optical Diagnostics and Sensing of Biological Fluids and Glucose and Cholesterol Monitoring II, Proc. SPIE* **4624**, 36–46 (2002).
20. Zaccanti, G., Bianco, S. D. and Martelli, F., "Measurements of optical properties of high-density media," *Appl. Opt.* **42**, 4023–4030 (2003).
21. Cheong, W. F., Prahl, S. A. and Welch, A. J., "A review of the optical properties of biological," *IEEE J. Quantum Electronics* **26**, 2166–2185 (1990).